

8-1-2014

## Analytical and Experimental Analysis of Magnetorheological Elastomers

Sarah Trabia

University of Nevada, Las Vegas, [trabias@unlv.nevada.edu](mailto:trabias@unlv.nevada.edu)

Follow this and additional works at: <https://digitalscholarship.unlv.edu/thesesdissertations>



Part of the [Engineering Science and Materials Commons](#), [Materials Science and Engineering Commons](#), and the [Mechanical Engineering Commons](#)

---

### Repository Citation

Trabia, Sarah, "Analytical and Experimental Analysis of Magnetorheological Elastomers" (2014). *UNLV Theses, Dissertations, Professional Papers, and Capstones*. 2221.  
<https://digitalscholarship.unlv.edu/thesesdissertations/2221>

This Thesis is protected by copyright and/or related rights. It has been brought to you by Digital Scholarship@UNLV with permission from the rights-holder(s). You are free to use this Thesis in any way that is permitted by the copyright and related rights legislation that applies to your use. For other uses you need to obtain permission from the rights-holder(s) directly, unless additional rights are indicated by a Creative Commons license in the record and/or on the work itself.

This Thesis has been accepted for inclusion in UNLV Theses, Dissertations, Professional Papers, and Capstones by an authorized administrator of Digital Scholarship@UNLV. For more information, please contact [digitalscholarship@unlv.edu](mailto:digitalscholarship@unlv.edu).

ANALYTICAL AND EXPERIMENTAL ANALYSIS OF  
MAGNETORHEOLOGICAL ELASTOMERS

By

Sarah Trabia

Bachelor of Science in Mechanical Engineering  
University of Nevada, Las Vegas  
2012

A thesis submitted in partial fulfillment of the requirements for the

Master of Science in Engineering – Mechanical Engineering

Department of Mechanical Engineering  
Howard R. Hughes College of Engineering  
The Graduate College

University of Nevada, Las Vegas  
August 2014



**THE GRADUATE COLLEGE**

We recommend the thesis prepared under our supervision by

**Sarah Trabia**

entitled

**Analytical and Experimental Analysis of Magnetorheological  
Elastomers**

is approved in partial fulfillment of the requirements for the degree of

**Master of Science in Engineering - Mechanical Engineering  
Department of Mechanical Engineering**

Woosoon Yim, Ph.D., Committee Chair

Kwang Kim, Ph.D., Committee Member

Brendan O'Toole, Ph.D., Committee Member

Rama Venkat, Ph.D., Graduate College Representative

Kathryn Hausbeck Korgan, Ph.D., Interim Dean of the Graduate College

**August 2014**

## Abstract

# ANALYTICAL AND EXPERIMENTAL ANALYSIS OF MAGNETORHEOLOGICAL ELASTOMERS

By  
Sarah Trabia

Dr. Woosoon Yim, Examination Committee Chair  
Professor of Mechanical Engineering  
University of Nevada, Las Vegas

Many engineering applications ranging from robotic joints to shock and vibration mitigation can benefit by incorporating components with variable stiffness. In addition, variable stiffness structures can provide haptic feedback (the sense of touch) to the user. In this work, it is proposed to study Magnetorheological Elastomers (MRE), where iron particles within the elastomer compound develop a dipole interaction energy, to be used in a device for haptic feedback. A novel feature of this MRE device is to introduce a field-induced variable shear modulus bias via a permanent magnet and using a current input to the electromagnetic control coil to change the modulus of the elastomer in both directions (softer or harder).

In this preliminary work, both computational and experimental results of the proposed MRE design are presented. The design is created in COMSOL to verify that the magnetic field is in the desired direction. MRE was fabricated and characterized using a Bose Dynamic Mechanical Analyzer for the shear modulus. Using this information, it is possible to know how the MRE will react in magnetic fields within the haptic feedback device.

Additionally, a model for an MRE is developed in a multi-physics COMSOL program that is linked to a MATLAB function that predicts the shear modulus and

incorporates it into the material properties to best simulate the MRE's ability to change shear modulus.

## Acknowledgements

I would like to thank my family for supporting me throughout my endeavors and anything I have wanted to accomplish. They are the reason that I push through and continue with my education. I would also like to thank Dr. Woosoon Yim for advising and guiding me through this process. Without his help, I would not have received the NASA Space Grant fellowship or learned so much.

# Table of Contents

Abstract .....	ii
Acknowledgements .....	v
List of Tables .....	vii
List of Figures .....	viii
Chapter 1: Introduction .....	1
1.1 Literature Review .....	1
1.2 Proposed Device .....	3
1.3 Objectives .....	4
1.4 Organization .....	5
Chapter 2: Fabrication and Characterization of the MRE .....	6
2.1 Materials .....	6
2.2 Fabrication .....	7
2.3 Characterization and Results .....	8
2.4 Discussion .....	13
Chapter 3: Device Design .....	15
3.1 Design Specifications .....	15
3.2 COMSOL Analysis .....	17
3.3 Final Design .....	24
3.4 Device Construction .....	26
Chapter 4: COMSOL Model of MRE Shear Modulus Change .....	28
4.1 Relation between Shear Modulus and Magnetic Field .....	28
4.2 MATLAB Function .....	30
4.3 COMSOL Model .....	31
4.4 Results .....	34
4.5 Discussion .....	36
Chapter 5: Conclusions and Future Work .....	37
5.1 Conclusions .....	37
5.2 Future Work .....	38
Appendix .....	40
Appendix A: MATLAB Code .....	40
Bibliography .....	43
Curriculum Vitae .....	44

## List of Tables

Table 1: The composition of prepared MR elastomers.....	7
Table 2: Conditions for Bose DMA test. ....	11
Table 3: Domain conditions for Magnetic Fields, No Currents.....	19
Table 4: Domain conditions for Magnetic Fields. ....	20
Table 5: Strength of field going through the MREs.....	24
Table 6: Strength of field going through the MREs, final design. ....	26
Table 7: Domain conditions.....	33
Table 8: Boundary Conditions. ....	34



## List of Figures

Figure 1: The morphology of CIPs measured by SEM.....	6
Figure 2: Set up for curing the MRE in magnetic field and heat. ....	8
Figure 3: SEM images of two MRE samples, without and with magnetic field.....	8
Figure 4: MRE sample being tested for shear modulus in DMA.....	10
Figure 5: Samples glued to aluminum sheet metal for testing.....	10
Figure 6: Results for Shear Modulus (Plot 1). ....	11
Figure 7: Results for Shear Modulus (Plot 2). ....	12
Figure 8: Test setup for varying magnetic field.....	13
Figure 9: Results for MRE with varying magnetic field.....	13
Figure 10: MRE device design. ....	16
Figure 11: Detailed view of the MRE rings around the aluminum tube.....	16
Figure 12: 2D Axisymmetric model for the device. ....	17
Figure 13: Desired Field Direction shown in red dashed lines. ....	18
Figure 14: Domain conditions for Magnetic Fields, No Currents. ....	19
Figure 15: Domain conditions for Magnetic Fields. ....	20
Figure 16: Mesh created for analysis. ....	21
Figure 17: Results for Magnetic Fields, No Current.....	22
Figure 18: Results for Magnetic Fields, with 0.5 Amps (against permanent magnet).....	22
Figure 19: Results for Magnetic Fields, with 0.5 Amps (with permanent magnet). ....	23
Figure 20: Results for Magnetic Fields, with 0.5 Amps (against permanent magnet).....	23
Figure 21: Results for Magnetic Fields, with -0.5 Amps (with permanent magnet).....	24
Figure 22: Results for Magnetic Fields, No Current (final design). ....	25
Figure 23: Results for Magnetic Fields with 0.5 Amps (against permanent magnet, final design). .....	25
Figure 24: Results for Magnetic Fields with -0.5 Amps (with permanent magnet, final design)..	26
Figure 25: Aluminum mold for the MRE. ....	27
Figure 26: Completed MRE device. ....	27
Figure 27: Diagram for variables, A is side view, B is top view (Chen et al., 2007). ....	29
Figure 28: Geometry of model, axis in $\mu\text{m}$ . ....	31
Figure 29: Mesh for model, axis in $\mu\text{m}$ . ....	32
Figure 30: Cut Point for data recording, axis in $\mu\text{m}$ . ....	32
Figure 31: Domain conditions. ....	33
Figure 32: Boundary Conditions.....	33
Figure 33: Calculated shear modulus using MATLAB function. ....	35
Figure 34: Displacement data. ....	35
Figure 35: Shear stress data. ....	36
Figure 36: Shear strain data. ....	36

## Chapter 1: Introduction

### 1.1 Literature Review

Today's technology has made it possible to control the motion of a large number of devices with a great level of precision. However, the state of this technology is still in a primitive stage when it comes to controlling the mechanical properties of a material. Variable Stiffness Joints (VSJ) are constructed in diverse ways. One joint uses ring shaped magnets that when rotated creates a torque that mimics a nonlinear spring (Park, 2008). To change the stiffness, the area between the two magnets is increased or decreased (Park, 2008). This method is limited to the specific application of a robot's joint, though it could be used for other uses of a similar nature. There are also VSJ that are made up of multiple pulleys and springs that are used in robotic prosthetics to produce a motion similar to that of human joints (Ham, 2009). These systems are successful at creating a more natural human-like movement, but are fairly complicated and bulky. The components must be perfectly aligned and move together in a prescribed manner to produce the motion needed. Another design uses a motor that turns a torsional spring to set the pre-set stiffness for the joint (Wolf, 2008). With the system that relies on a motor, it is often difficult to achieve a precise control of the stiffness since it can affect position accuracy. These different systems are a good first step towards controlling stiffness, but may not be the best solution for simultaneous control of both position and stiffness of mechanical joints. It may be best to look for a way to directly control stiffness, rather than creating the stiffness needed.

There are materials available that have the ability to change their mechanical properties, which are called smart or active materials. One of these actively controllable

materials is the Magnetorheological Elastomer (MRE) which can change its stiffness subject to externally applied electromagnetic flux. A similar material called Magnetorheological Fluid (MR Fluid) is a liquid that is made up of silicone oil and micron-sized iron particles (Ruddy, 2012). When a magnetic field is present, the iron particles line up and the viscosity of the MR Fluid changes. Similarly, MRE is a silicone polymer with micron-sized iron particles embedded in it as the active component. The MRE should be cured in a magnetic field so that the iron particles align in the correct orientation to ensure that the stiffness change is in the desired direction (Ruddy, 2012). One advantage to MREs is that there is no chance of particle settling (an issue common with MR Fluids), since they are suspended in their position within the polymer (Liao, 2012). When a magnetic field is present, the material can change its stiffness depending on the direction of the field. By designing a device that could control the strength of the magnetic field, it would be possible to control the stiffness of the material. This could allow the MREs to be incorporated in different applications where variable stiffness feature is needed.

Some of the applications for MREs are used in vehicles. There are automotive bushings and engine mounts that utilize MREs to control the stiffness (Ruddy, 2012). The automotive bushings, which were patented by Ford Motor Company, are used to lower the effect of resonances in the suspension system caused by excitation due to torque differences from worn brake rotors (Kallio, 2005). They have also been tested in vibration isolation by various researchers. One device used a load cell to find the force applied to the MRE and adjusted the magnetic field accordingly to ensure the correct stiffness was introduced to absorb the force (Opie, 2012). The device was successful in

accurately adjusting the stiffness using a combination of flux sensor, load cell, and isolate the payload for vibration (Opie, 2012). Another application for MREs as vibration isolation is within the driveline assemblies of vehicles, where the MRE is used as a damper to absorb vibrations (Li, 2008).

## 1.2 Proposed Device

The proposed device will be a miniaturization of the device design by Opie (Opie, 2008). The original device is about 6 lbs. and requires 2 Amps to power the coil. The new device will be smaller, but use the same general idea to create a magnetic field through the MRE. By designing the device in COMSOL (finite element analysis), it gives the possibility of trying different geometries and materials to find the best design, without purchasing and building many devices. Opie's device is a good first step towards creating a device that can control the shear modulus of the MRE.

This device can present a potential breakthrough in designing robotic manipulators. The potential application of the new device will involve haptic, or tactile, devices, where the MRE can be incorporated in the interface of the tele-operator, such as an astronaut or a surgeon, to provide a tactile feedback from the robot by changing the stiffness of the MRE in real time. For example, the user of a robot that is operated from a different location could tell whether the robot has collided with an object by receiving feedback from a pressure sensor in the form of the MRE stiffening. Controlling robots by tele-operation could become even more effective if the user were to gain more information about the robot itself and its environment, since this can be difficult by using only cameras. Another goal of this thesis is to design a small device that is still able to

produce a strong enough field to change the stiffness of the MRE because of the applications that have been predetermined. Also, if it is possible to design a small MRE device, it could be applied in many different applications other than the ones stated.

The proposed device will be applicable for the haptic device. It can be used in any system. Since the device is designed in COMSOL, it can be created specifically for haptic feedback. The device is best for this application because it can be tailored for any size. It will give the user the flexibility to design a device that can fit their needs for a haptic feedback.

A device that is similar to the one above is a MR Fluid haptic brake system (Kosasih et al, 2006). It uses a joystick that the user can move and will feel resistance. The device uses a coil within a case that also holds the MR Fluid and rotary disc, to create the magnetic field to change the viscosity of the fluid. The device is successful in creating a haptic device, but it only uses the haptic feedback to verify that the brake system is working correctly, not for actual haptic feedback. The proposed device will be creating an MRE haptic device that will be using the feedback as a major component in the device.

### 1.3 Objectives

The objective of this research is to analyze the feasibility of using MRE in a haptic feedback application. Since this type of application has not been tried before, there are some points that need to be researched, such as how reactive the MRE should be to magnetic fields. In order for a user to feel a difference, the MRE used would need to change its shear modulus significantly. The device that produces the magnetic field for

such an application will need to be small, allowing it to be used in surfaces and other places where haptic feedback could be used. The shape, size, and type of device that will be used in haptic feedback will be explored to find the best way to produce a field needed for the MRE. An additional objective is to fully understand how an MRE will react in different field strengths. Knowing how different kinds of MRE will change in various fields is important to finding the best composition for a haptic feedback application.

With the objectives stated and the goals set for finding an MRE for haptic feedback, the contributions of this thesis are:

- the design of an MRE with a large range of stiffness variation,
- the miniaturization of a previous MRE device,
- and the creation of a COMSOL and MATLAB model to predict the reaction of the material under a given magnetic field.

## 1.4 Organization

In this thesis, multiple aspects of the project will be explored. It will begin with the creation and characterization of the MRE in Chapter 2. Chapter 3 will show the design process for miniaturization of the device designed by Opie (Opie, 2008) using COMSOL and the building of the new device. Chapter 4 will present a COMSOL model of MRE showing the ability to predict the change in shear modulus due to the magnetic field present.

## Chapter 2: Fabrication and Characterization of the MRE

Before designing a device, it is necessary to have an MRE designed to the desired initial specifications. It would be beneficial to have the MRE begin with a low stiffness so that the stiffness change will have a larger range. Another reason for why the MRE needs to be initially soft is because there will be a permanent magnet within the device to pre-strain the MRE and give it a preliminary stiffness before the coil is turned on to increase or decrease it.

### 2.1 Materials

The silicone resin and curing agent (R-2652) were purchased from NuSil Technology®. Carbonic iron particles (CIPs: FE006045) were prepared from Goodfellow®, Figure 1. Toluene as a solvent and 3-glycidyloxypropyltrimethoxysilane (GPTMS) as a silane coupling agent were purchased from Sigma-Aldrich. The silane coupling agent is used to ensure that the iron particles bond well with the silicone so that they stay in the assigned line up. This has been shown as a benefit by Wu to improve the stability of the iron particles (Wu et al, 2009).

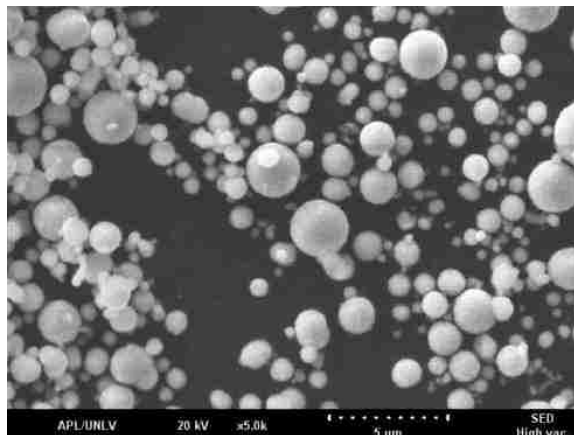


Figure 1: The morphology of CIPs measured by SEM.

## 2.2 Fabrication

First, GPTMS was dissolved in toluene at 60 °C for 1 hour and then CIPs were added and modified in the prepared solution at 80 °C for 3 hours. Then, the silicone resin was added and dissolved at 60 °C for an hour. The curing agent was then added into the mixture and applied vacuum to remove bubbles in the mixture for 30 minutes. Finally, the viscous mixture was poured into a mold and cured in an oven at 90 °C for two hours. The main composition of all samples can be seen in Table 1.

To make the Pristine Gel 8170 sample, Part A and Part B are mixed in a 1:1 ratio and cured at 90 °C for two hours.

**Table 1: The composition of prepared MR elastomers.**

<b>Composition</b>	<b>0 vol.% of CIP</b>	<b>15 vol.% of CIP</b>
Silicone Resin (ml)	20	17
Curing agent (ml)	2	1.7
CIPs (ml)	-	3
Toluene (ml)	10	8.5
Modified by GPTMS (ml)	-	3

To align the iron particles in the MRE, two coils are used. This process is called poling. They are put into an oven, Lindberg/Blue UT150, with a power source nearby (Figure 2). A current of 0.1 Amps is fed to the coils to produce a field of about 60 mT. The MRE is poured into a mold and put into space between the coils to be cured in the field. The oven is set to 95°C and the MRE is allowed to cure overnight. The SEM, Figure 3, verifies that iron particles have aligned by comparing two samples of MRE, without and with magnetic curing. It can be seen that the iron particles on left hand side are haphazardly located throughout the silicone, due to the lack of magnetic field during curing. The presence of the field is shown on the right hand side because the iron particles have lined up almost vertically.





Figure 2: Set up for curing the MRE in magnetic field and heat.

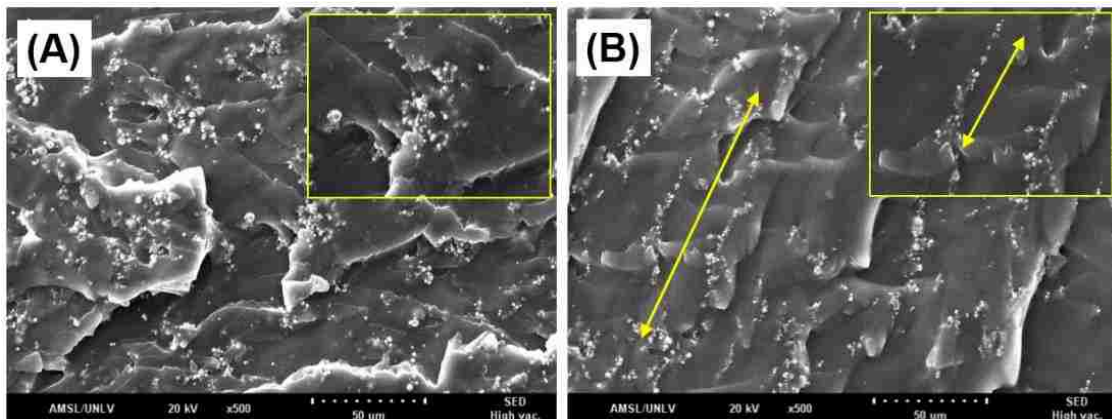


Figure 3: SEM images of two MRE samples, without and with magnetic field.

### 2.3 Characterization and Results

Bose Dynamic Mechanical Analyzer was used to identify the shear modulus of the MREs, as well as Neoprene (a rubber sheet with a known shear modulus), a sample of R-2652, and another silicone base, Gel 8170. A fixture was printed to induce shear force on the samples, Figure 4. It is stiff enough to handle the forces during the test and transfer the reaction forces fully to the load cell. The fixture had two pieces of aluminum sheet

metal that can be attached to it. This is where the samples will be glued to ensure that slipping does not occur during the experiment, Figure 5. Each sample is cut into 10 mm x 10 mm x 5 mm pieces. The samples were tested under four frequencies (0.1, 1, 10, 100 Hz) with an amplitude of 0.4 mm. To ensure accuracy and consistency of the results, the following steps were taken:

- All the samples are weighed and measured with a caliper to note the actual dimensions.
- Each sample is glued to the aluminum sheet metal pieces and left overnight to dry.
- When the specimen is mounted into the machine, the compressed thickness is measured with a caliper to be sure that the correct value is entered into Win7 program that processes the data.
- An initial displacement of 1 mm is input so all the measurements begin at the same reference point.
- Each sample is tested four times consecutively, without removing the sample, to see if the values are consistent with the same setup.



Figure 4: MRE sample being tested for shear modulus in DMA.



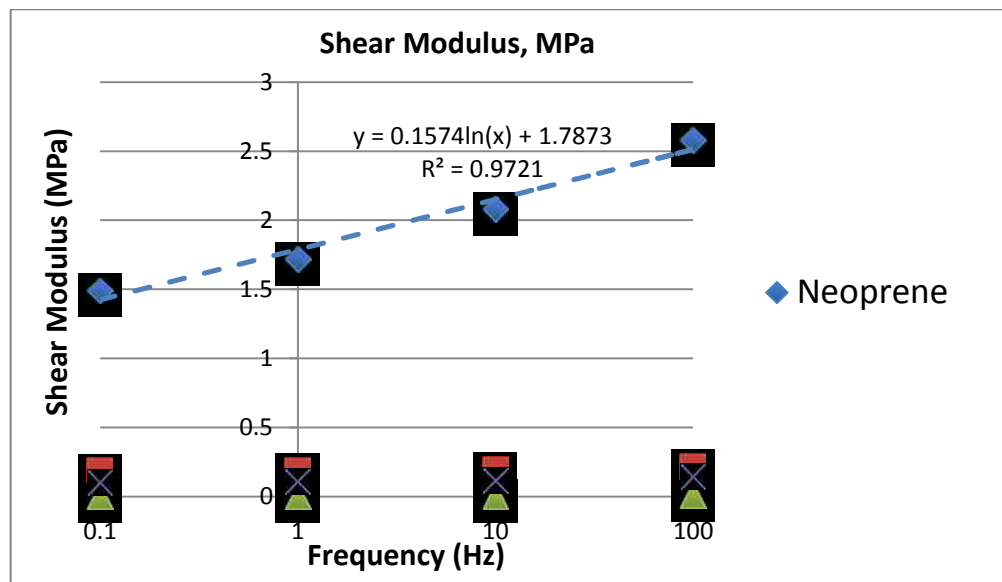
Figure 5: Samples glued to aluminum sheet metal for testing.

Table 2 shows the conditions for the shear modulus testing. Each sample undergoes the same testing conditions. The first phase of testing was for the initial values of shear modulus (with no magnetic field present). The results are shown in Figure 6. Neoprene is significantly higher than the rest causing the results for the three other samples to be difficult to interpret. They are plotted together in Figure 7 for a better representation. Neoprene has a shear modulus that ranges between 1.5-3 MPa. The results shown in Figure 6 verify this. In the second plot (Figure 7), the three other samples are

plotted together to better compare the results. Gel 8170 is the softest of the materials tested and has the lowest initial shear modulus. Pristine Silicone (R-2652) has the highest shear modulus of the three samples and is very stiff to touch. MRE's initial shear modulus is slightly lower than the Pristine Silicone. This could be because of the ratios of the base silicone, solvent, silane agent, and the iron particles.

**Table 2: Conditions for Bose DMA test.**

Condition Number	Frequency, Hz	Mean Level, mm	Dwell at Mean, sec	Dynamic Amplitude, mm	Hold Value, mm	Hold Value Dwell, sec
1	0.1	-0.4	1	0.4	-0.2	1
2	1	-0.4	1	0.4	-0.2	1
3	10	-0.4	1	0.4	-0.2	1
4	100	-0.4	1	0.4	-0.2	1



**Figure 6: Results for Shear Modulus (Plot 1).**

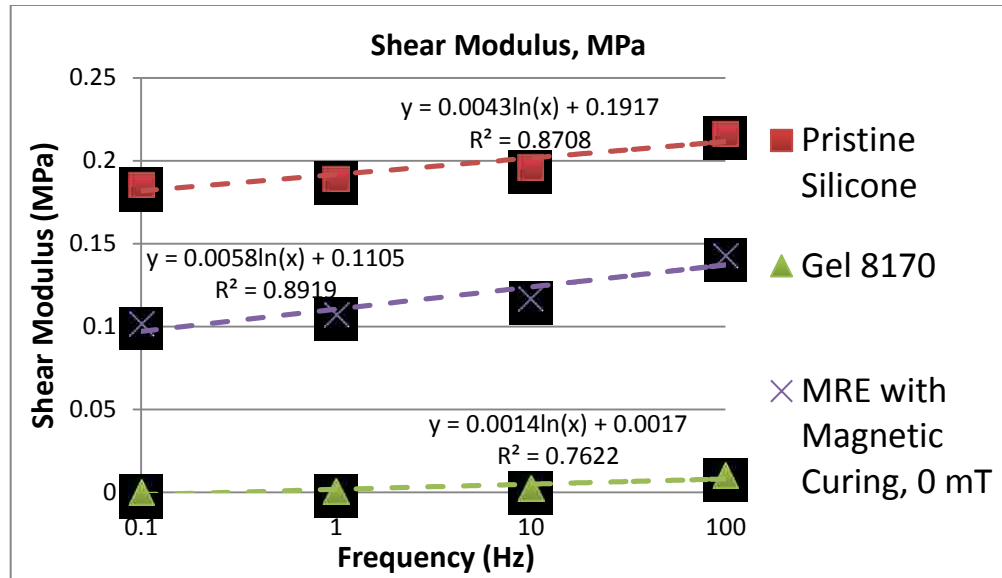


Figure 7: Results for Shear Modulus (Plot 2).

The second phase of testing involves applying a magnetic field to cause shear modulus change. This is done by using two 2000 turn coils made with 14 AWG wire. They are placed around the testing fixture and produce a field that moves through the aligned iron particles (Figure 8). The field varies from 0 mT to 300 mT, in increments of 100 mT. The results are shown in Figure 9. The maximum percent change in shear modulus is about 17%, which would be undiscernible to touch for a user. The desired MRE should have at least 50% change. The cause for such a low percent change could be because the base of the MRE, the silicone R-2652, is stiff to begin with. It may be more useful to use silicone with a low shear modulus as the base.



Figure 8: Test setup for varying magnetic field.

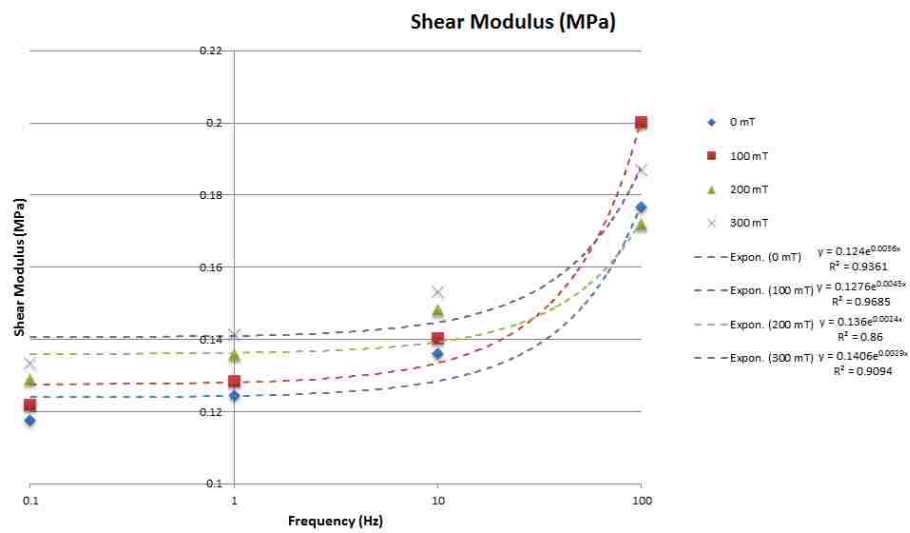


Figure 9: Results for MRE with varying magnetic field.

## 2.4 Discussion

The MRE fabricated is successful in changing when a magnetic field is present. It could be used in applications where low shear modulus changes are needed. However, it is important to find a silicone with a low shear modulus for haptic feedback application. This will give the material the ability to have a larger stiffness change. The base silicone will still need to be able to be strong enough to hold the iron particles in a defined alignment after it has been cured. If its viscosity is very low, then the MRE will act more

as an MR fluid. This will cause the material to be not useful in a haptic feedback device because it will cause many issues such as leakage and non-uniform distribution of iron particles.

Another issue to work out is a better way to both heat and poling the MRE. The current setup needs a large air gap to fit the sample. This requires a large input of current to produce a large enough magnetic field. In addition, if the field is too strong, the iron particles would be pulled out of the silicone. On the other hand, it is necessary to have a strong field to get the best alignment within the material. These issues could also be solved by using a different silicone base, but also the uses of molds and heat tapes to cure the MRE could help.

## Chapter 3: Device Design

A device that can produce a magnetic field through the MRE is needed for any application. The novel feature of this design is adding a permanent magnet to pre-strain the MRE, allowing the user to both increase and decrease the material's shear modulus. This can open new areas of applications for MREs, which do not naturally have the ability to become softer. If the device is designed to be small enough, it can be later applied to a large variable stiffness surface.

### 3.1 Design Specifications

In order to design the device, some specifications are defined. The device:

- needs to be small and portable,
- should not need a large power source to operate,
- need some kind of shielding so that the magnetic field does not interfere with anything around it,
- need to be a permanent magnet in the device to pre-strain the MRE,
- need a core in the center of the device to facilitate the motion of the field,
- and need a coil that will either counteract or assist the permanent magnet's field to adjust the stiffness accordingly.

With the following requirements in mind, a general design is presented, Figure 10. The permanent magnet is used to pre-strain the MRE. The coil, put within the magnet to direct the field in the same direction as the magnet, will be used to either assist or go against the magnet to increase or decrease the stiffness of the MRE. Magnetic shielding is used to keep the field within the device. The MRE rings hold the aluminum tube, Figure



11. The aluminum tube and plate are where the force will be applied. Changes in shear modulus of the MRE will affect the ease or difficulty of applying the force. There is a small gap of air below the MRE rings to allow for some movement, Figure 11. A core is placed in the center of the device to ensure that the field flows through the center and back through the magnet with only a small amount of losses.

The main component of the device is the permanent magnet. A magnet (DM 865) was obtained from DuraMag with magnetic coercive force of 143 kA/m. All of the other dimensions of the device were adjusted to fit around this magnet.

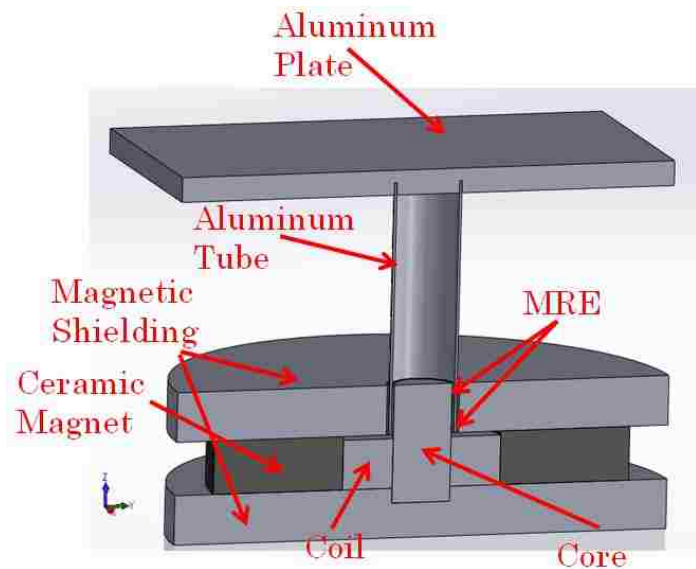


Figure 10: MRE device design.

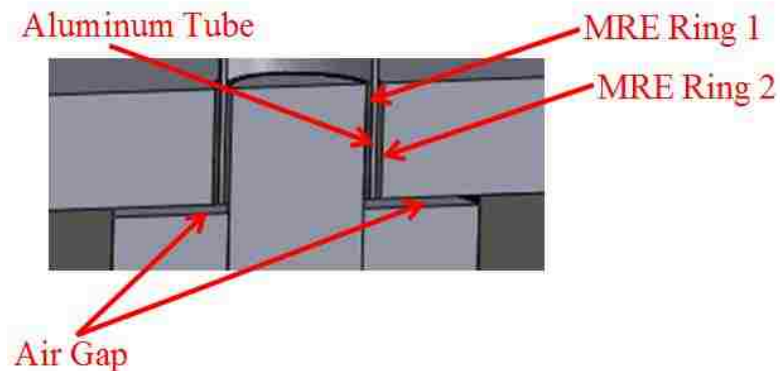


Figure 11: Detailed view of the MRE rings around the aluminum tube.

### 3.2 COMSOL Analysis

The device is tested in a finite element analysis software called COMSOL 4.3b. To simplify the analysis, a 2D axisymmetric model was used (Figure 12). The semicircle around the device is used to represent the air. This model was tested to find the number of turns in the coil necessary to counteract the permanent magnet as well as the thickness of the magnetic shielding needed. All of the material characteristics are starting points. The MRE permeability is set to 2 (Opie, 2011). Those values will be updated in the COMSOL analysis, once everything is finalized. A core with a high permeability of 600,000 is used in the center of the device. For the magnetic shielding, a low carbon steel (AISI 1010) is needed to be good at shielding. The BH and HB curve for a low carbon steel is added to the material property so that COMSOL understands it acts as a shield. “Potting material” is used to model a multi-turn coil in COMSOL.

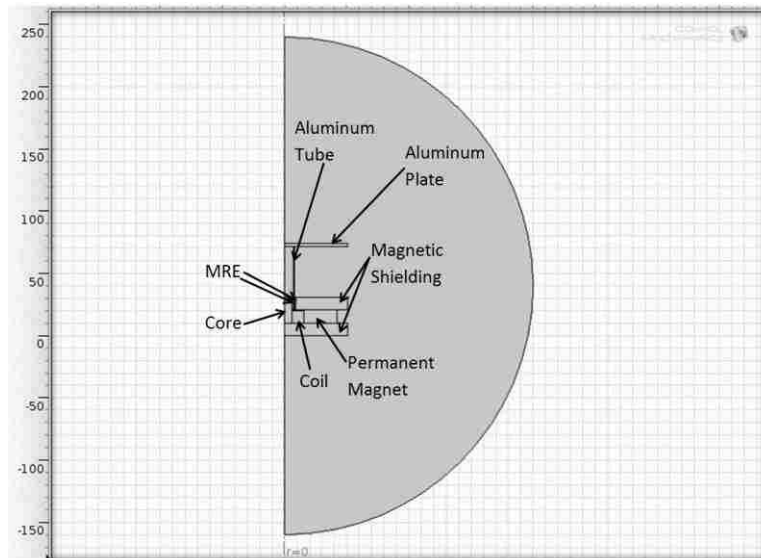


Figure 12: 2D Axisymmetric model for the device.

Once all of the material properties have been included, the physical loads need to be applied. For this analysis, Magnetic Fields (No Current) and Magnetic Fields with a

Multi-Turn Coil were applied to the device. The governing equations for Magnetic Fields (No Current) are

$$\nabla \cdot (\mu_0 \mu_r H) = 0$$

$$H = -\nabla V_m + H_b$$

$$H = -\nabla V_m.$$

For Magnetic Fields with a Multi-Turn Coil, those equations are:

$$\nabla \times H = J_e$$

$$B = \nabla \times A$$

$$\nabla \times (\mu_0^{-1} \mu_r^{-1} B) - \sigma v \times B = J_e.$$

It is necessary to analyze without current to see how much the permanent magnet pre-strains the MRE. Initial testing will make sure that the device is able to make a uniform field throughout the MRE to ensure that there is a uniform stiffness change. Figure 13 shows the desired field path throughout the device. This field path needs to be possible in both without and with current.

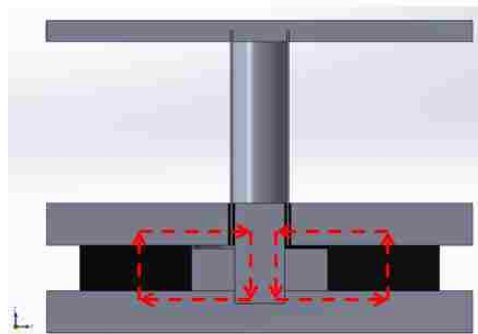


**Figure 13: Desired Field Direction shown in red dashed lines.**

The boundary and domain conditions for the physics of Magnetic Fields, No current are shown through Figure 14 and Table 3. The main point to note is the

differences in “Magnetic Flux Conservation” that are applied. Each is unique for the type of material. It is important to be sure to do this in COMSOL so that it can be able to differ and best represent each part of the device.

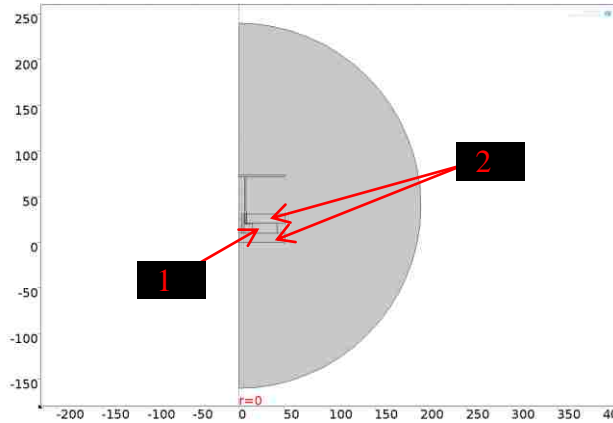


Figure 14: Domain conditions for Magnetic Fields, No Currents.

Table 3: Domain conditions for Magnetic Fields, No Currents.

Domains	Condition	Magnetic Field
All except 1 and 2	Magnetic Flux Conservation 1	Relative permeability (from material)
1	Magnetic Flux Conservation 2	Magnetization ( $z = 143 \text{ kA/m}$ )
2	Magnetic Flux Conservation 3	BH curve (from material card)

For Magnetic Fields, current is being applied so now the condition applied will be “Ampere’s Law.” Again, each is specific for the type of material and must be applied in each condition to best simulate the device while current is being applied. The conditions are shown through Figure 15 and Table 4. The coil is given a different condition called “Multi-Turn Coil.” In this condition, the user can specify the number of turns, coil conductivity, wire gauge, and the current applied.

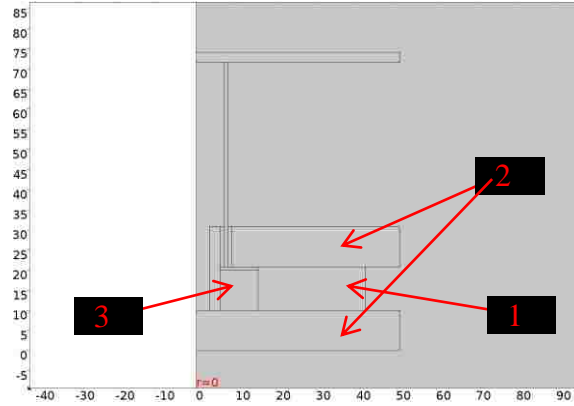


Figure 15: Domain conditions for Magnetic Fields.

Table 4: Domain conditions for Magnetic Fields.

Domains	Condition	Magnetic Field
All except 1, 2, and 3	Ampere's Law 1	Relative permeability (from material)
1	Ampere's Law 2	Magnetization ( $z = 143 \text{ kA/m}$ )
2	Ampere's Law 3	HB curve (from material card)
3	Multi-Turn Coil	$N$ (number of turns)=750; $\sigma_{coil}$ (coil conductivity) = $6e7 \text{ S/m}$ ; AWG (American Wire Gauge) = 28.

The mesh created has 4781 elements and the element size range is from 1 mm to 20 mm, Figure 16. Within the device, the elements are constrained to be 1 mm to get accurate results, while the air around the device is allowed to range from 1 to 20 mm. This allows the results around the device to be very accurate. The further away the elements are from the device, the bigger they get which allows for a shorter run time. This was done through mesh stability. The element size for the air was adjusted until the best sizes were found that gives consistent results.

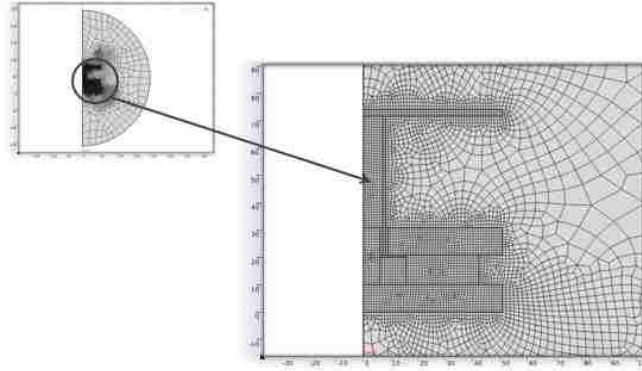


Figure 16: Mesh created for analysis.

For the first test, the analysis is run with Magnetic Fields (No Current) and the results are shown in Figure 17. This is how the device will be at rest. The goal of the next simulation is to see how many coil turns are needed to successfully counteract the permanent magnet. A parametric sweep is applied to the turns of the coil, giving the results for each iteration. From the design specifications, a maximum of  $\pm 0.5$  Amps will be used to ensure that the system does not overheat and to allow the use of a small power source. The values are collected and shown in the plots below (Figure 18 and Figure 19), where MRE 1 is the inner ring and MRE 2 is the outer ring. Keeping in mind that there is a small amount of space to work with, a high number of turns will not be possible. After some consideration of the data, 750 turns was chosen because this value is able to counteract the magnet sufficiently in the positive direction while aiding it in the negative direction to create significant differences in the strength of field. After applying the 750 turns to the coil, the results are shown in Figure 20 and Figure 21. The coil counteracts the permanent magnet (Figure 20) causing the field to be close to zero, which causes the MRE to be softer than it was initially. When the coil works with the permanent magnet

(Figure 21), the strength of the field increases causing the MRE to stiffen. The values of the fields in each MRE ring are presented in Table 5.

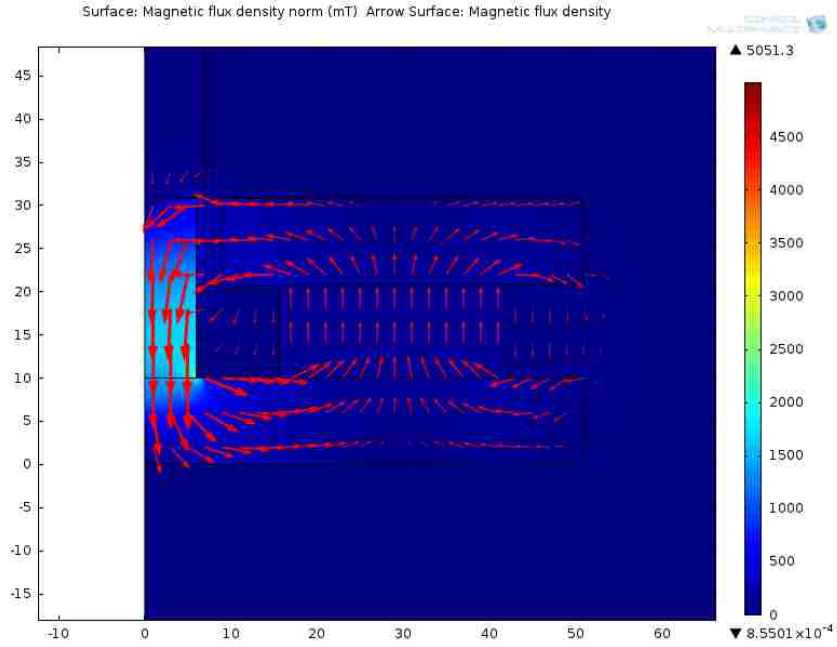


Figure 17: Results for Magnetic Fields, No Current.

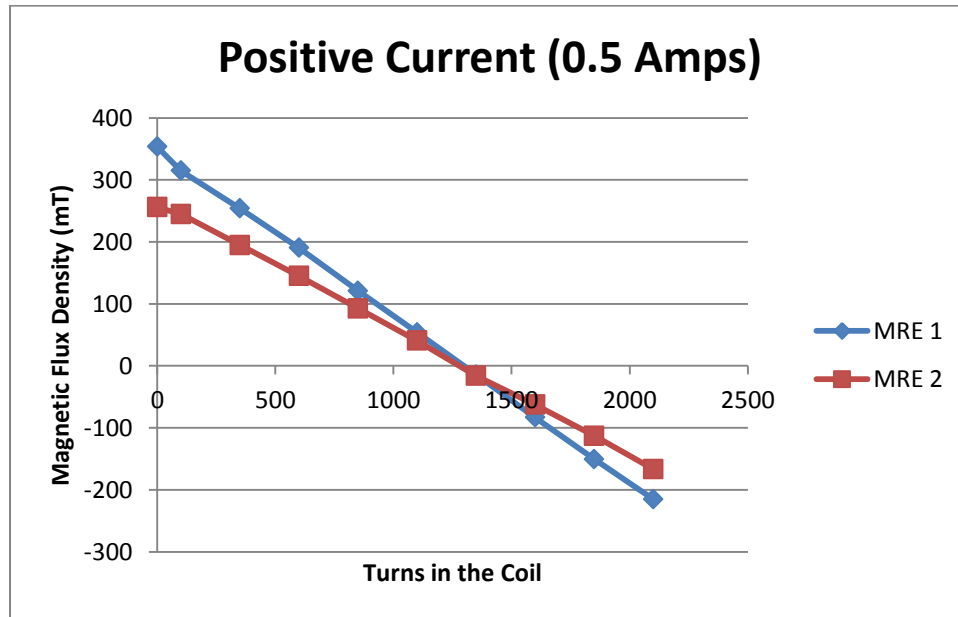


Figure 18: Results for Magnetic Fields, with 0.5 Amps (against permanent magnet).

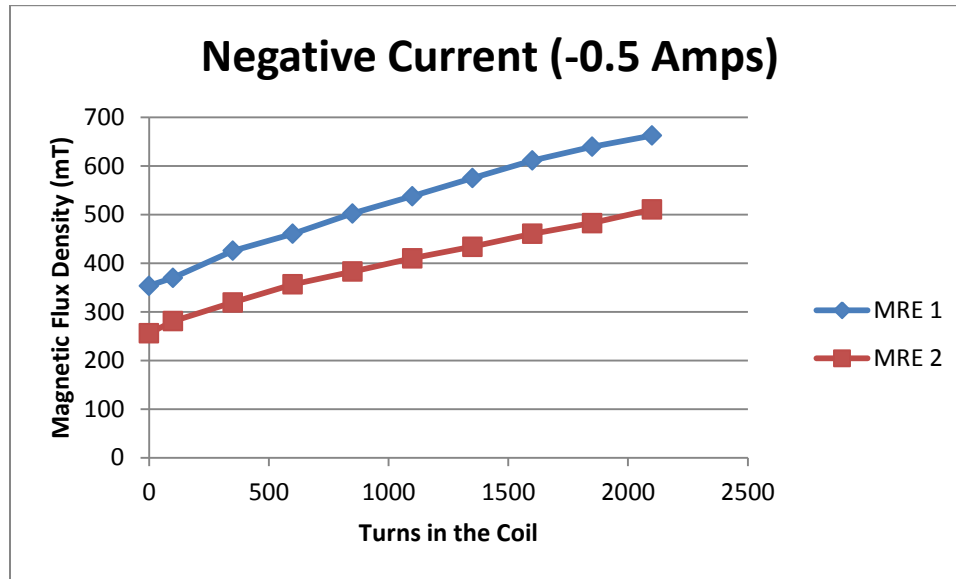


Figure 19: Results for Magnetic Fields, with 0.5 Amps (with permanent magnet).

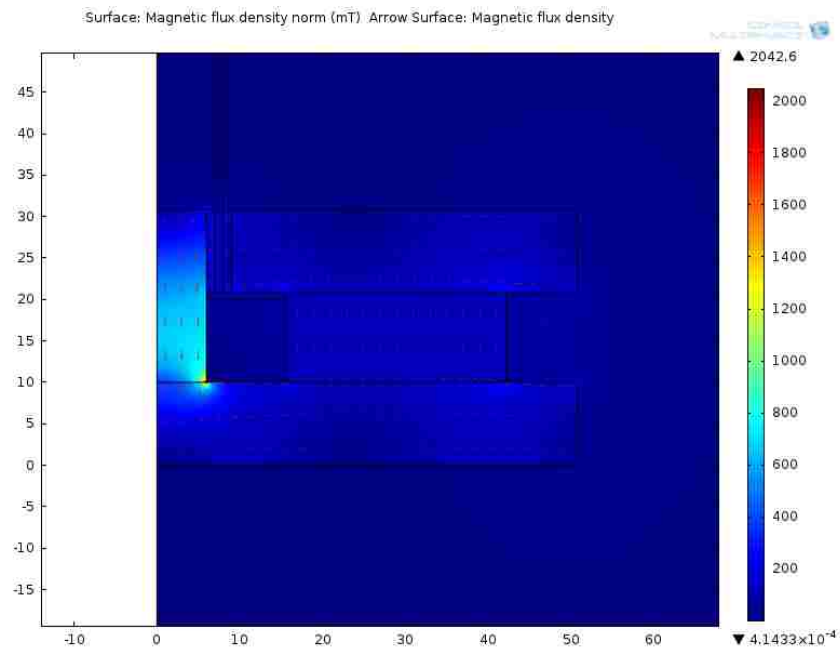


Figure 20: Results for Magnetic Fields, with 0.5 Amps (against permanent magnet).



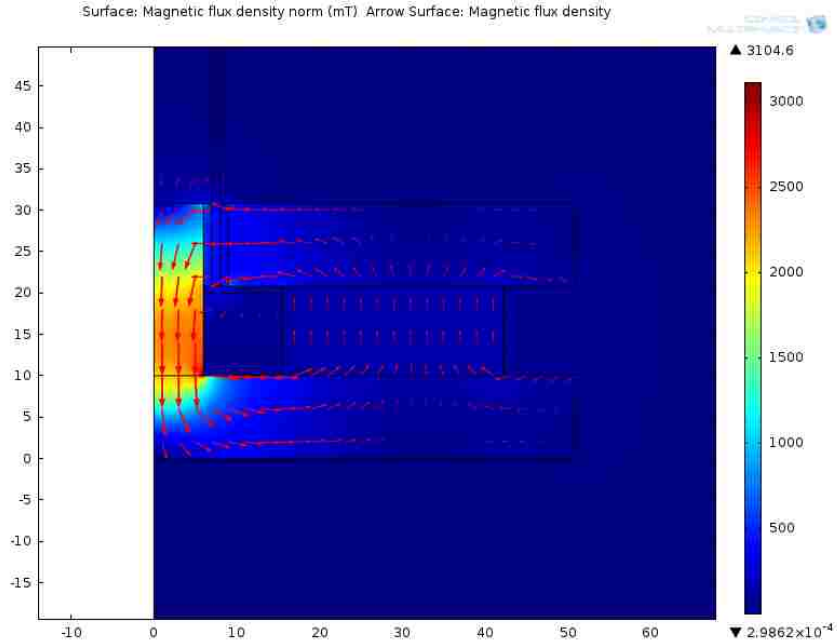


Figure 21: Results for Magnetic Fields, with -0.5 Amps (with permanent magnet).

Table 5: Strength of field going through the MREs.

	MRE 1 (mT)	MRE 2 (mT)
<b>No Current</b>	361.98	269.47
<b>0.5 Amps (Against Permanent Magnet)</b>	152.42	111.13
<b>-0.5 Amps (With Permanent Magnet)</b>	489.34	373.81

### 3.3 Final Design

The parts for the device were finalized depending on the results from section 3.2 as well as what was available on the market. The coils are 750 turns of 28 AWG, custom made from Custom Coils. The cores (C055125A2) have a permeability of 300,000 and were purchased from MTL distribution. The steel plates were adjusted to AISI 1018 from McMaster-Carr. After updating the COMSOL model with the parts and MRE characteristics, the design was tested again to verify that the design will work. The results of the fields are shown in Figure 22, Figure 23, and Figure 24. The values of the magnetic field are shown in Table 6.

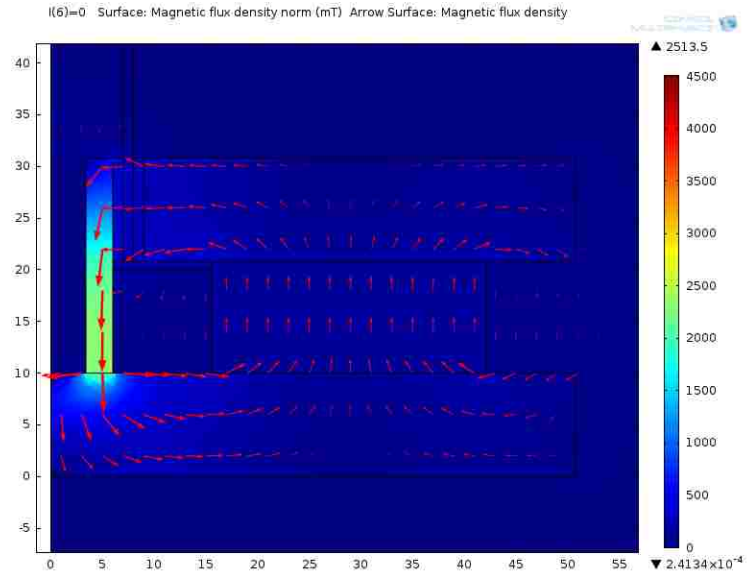


Figure 22: Results for Magnetic Fields, No Current (final design).

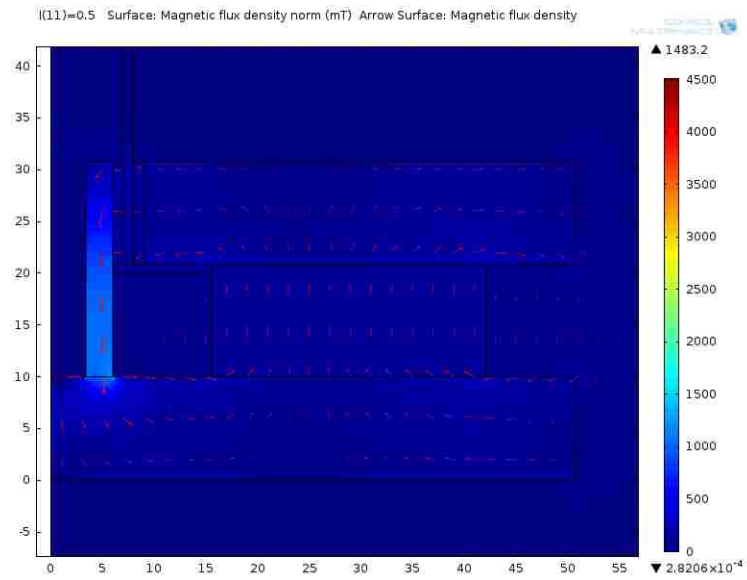


Figure 23: Results for Magnetic Fields with 0.5 Amps (against permanent magnet, final design).

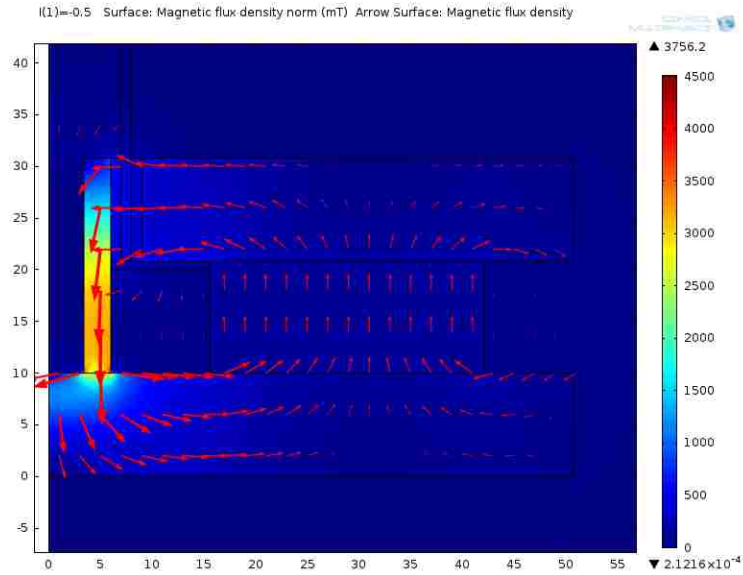


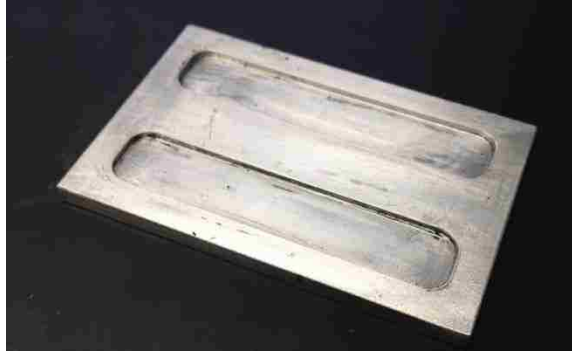
Figure 24: Results for Magnetic Fields with -0.5 Amps (with permanent magnet, final design).

Table 6: Strength of field going through the MREs, final design.

	MRE 1 (mT)	MRE 2 (mT)
<b>No Current</b>	328.3359	246.3115
<b>0.5 Amps (Against Permanent Magnet)</b>	145.945	111.028
<b>-0.5 Amps (With Permanent Magnet)</b>	454.5832	343.109

### 3.4 Device Construction

The MRE was made using the mold shown in Figure 25 and went through the same poling process as the samples. The device is built with all of the parts purchased. The MRE was glued to the surfaces using Loctite Super Glue®. The permanent magnet is strong enough to keep everything together without the need for bolts. The completed device is shown in Figure 26.



**Figure 25: Aluminum mold for the MRE.**

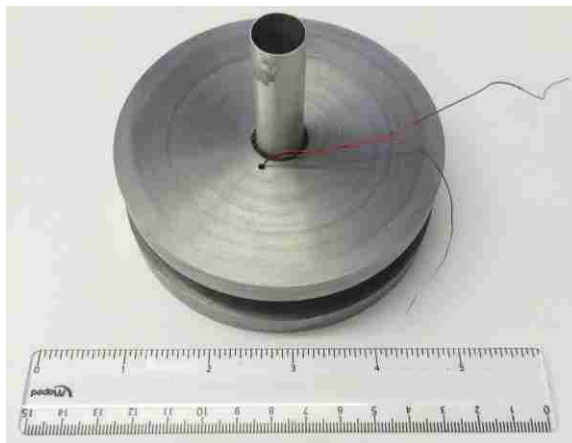


**Figure 26: Completed MRE device.**

The weight of the device is 3 lbs., making it more portable than the original device. The shape of the device is still bulky, making it difficult to fit in to certain applications, such as within remote controllers for robots or in the tools of surgeons. One way to reduce the weight and size of the device would be to find lighter magnetic shielding because this is the heaviest part of the device. A more cylindrical magnet could help with the shape of the device and allow it to be more streamlined. The need for a magnet could be eliminated by adding magnetic powder in the MRE composition, causing the MRE to pre-strain itself.

## Chapter 4: COMSOL Model of MRE Shear Modulus Change

A finite element analysis model of an MRE that can predict the shear modulus due to the magnetic field present could be very useful in the design of the material. It can help find the best combinations of silicone base, percent volume of iron particles, and magnetic field present during curing. To do this, COMSOL with MATLAB LiveLink™ is used to combine the simulation and multi-physics of COMSOL with the ease of creating a function for shear modulus in MATLAB. The two programs work together to calculate the shear modulus, then apply it to the material card of MRE and calculate all of the necessary equations to find the deformation of the material.

### 4.1 Relation between Shear Modulus and Magnetic Field

First, it was necessary to find the relation between shear modulus and Magnetic Field. Chen derived a relationship between the two by using SEM images of the cross sections and calculating different permeabilities to eventually find the shear modulus due to the magnetic field present (Chen et al, 2007). The derivations begin with the relationship between particle columns and the spaces between them:

$$\sum \frac{k_i}{L} = \frac{6\phi}{\left[\pi \left(\frac{nd}{m}\right)^2\right]}$$

where  $\phi$  is the volume percent of iron particles in the MRE sample,  $n$  is the number of aggregated particles,  $d$  is the diameter of the particles,  $m$  is the space between the columns,  $\sum k_i$  is the columns' total length, and  $L$  is the overall length of the sample (shown in Figure 27). Depending on the strength of the field during curing, the particles will align differently. The lower the field, the more sporadic the particles will be. The higher the field, the more organized the particles will become.

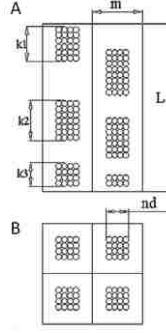


Figure 27: Diagram for variables, A is side view, B is top view (Chen et al., 2007).

The next portion deals with creating the permeabilities for the final equation. It

should be noted that there are two types of materials in the MRE: silicone and iron. Each material has its own permeability and it should be taken into effect. To find the effective magnetic permeability of the MRE, the following is used:

$$\mu_{matrix} = \mu_m = 2$$

$$\mu_{particles} = \mu_p = 1000$$

$$\mu_{pu} = \mu_m + \frac{2f\mu_m(\mu_p - \mu_m)}{[\mu_p + \mu_m - f(\mu_p - \mu_m)]}$$

where  $f=\pi/6$  (the ratio of the volumes) . The permeability is then broken down into two types: parallel to the column and perpendicular to the column. For the parallel permeability:

$$\mu_{||} = \frac{\mu_{12}\mu_m}{\left[ \left( \sum \frac{k_i}{L} \right) \mu_m + \left( 1 - \sum \frac{k_i}{L} \right) \mu_{12} \right]}$$

where  $\mu_{12}$  is the volumes connected in the parallel direction and shown as:

$$\mu_{12} = \left( \frac{nd}{m} \right)^2 \mu_{pu} + \left[ 1 - \left( \frac{nd}{m} \right)^2 \right] \mu_m$$

For the perpendicular permeability:

$$\mu_{\perp} = \left( \sum \frac{k_i}{L} \right) \mu_a + \left( 1 - \sum \frac{k_i}{L} \right) \mu_m$$

where:

$$\mu_b = \frac{\mu_{pu}\mu_m}{\left[\left(\frac{nd}{m}\right)\mu_m + \left(1 - \frac{nd}{m}\right)\mu_{pu}\right]}$$

$$\mu_a = \left(\frac{nd}{m}\right)\mu_b + \left(1 - \frac{nd}{m}\right)\mu_m.$$

Finally, the shear modulus can be expressed as:

$$G = \frac{(\mu_{\parallel} - \mu_{\perp})H_0^2 \sin \theta \cos \theta}{\theta}$$

where  $H_0$  is the magnetic field in A/m and  $\theta$  is the shear strain.

## 4.2 MATLAB Function

The MATLAB function calculates all of the equations above. The full code is shown in the appendix. The constants are given and labeled with comments to help with editing and adjusting values later on. The input for the function is the magnetic flux in A/m (B). For the shear strain, a simpler model where the shear modulus does not change is used. The shear strain is recorded and used as an assumption for what the shear strain could be when the shear modulus is changing. Depending on the magnetic field that COMSOL is inputting, it will run through an if-else statement to find the right shear strain to apply to the equation for shear modulus. For the case where there is no magnetic field present, the function is written to use 0.101 MPa, a value found experimentally with the DMA.

### 4.3 COMSOL Model

Two simple models are created with two permanent magnets and the MRE with air surrounding them, Figure 28. Two magnets are needed to direct the field uniformly through the MRE causing shear to the material. The materials added to the model were air (built in), ceramic magnet (user defined), and MRE (user defined). For one of the models, within the MRE material card, the input for shear modulus is the function written in MATLAB. The other model, 0.101 MPa was input for the shear modulus, which is the experimental value for shear modulus. The mesh is shown in Figure 29. The magnet and MRE mesh elements were constrained to a certain size (75  $\mu\text{m}$  for the magnets and 50  $\mu\text{m}$  for the MRE) and the air mesh elements were allowed to range from small (75  $\mu\text{m}$ ) to very large (500  $\mu\text{m}$ ) elements. The mesh has 13,839 quadrilateral elements. Since the model is fairly complex, this will help with cutting down the time needed to run the model. In order to compare the two models, a Cut Point is applied at the top left hand corner of the MRE (Figure 30), which records the data at that point in each iteration.

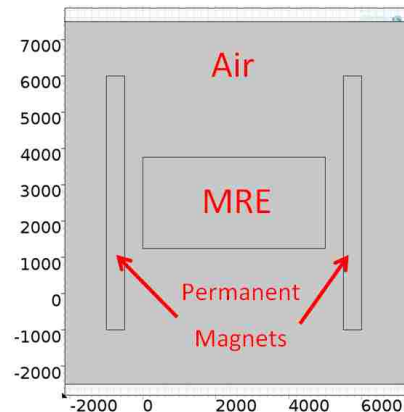


Figure 28: Geometry of model, axis in  $\mu\text{m}$ .



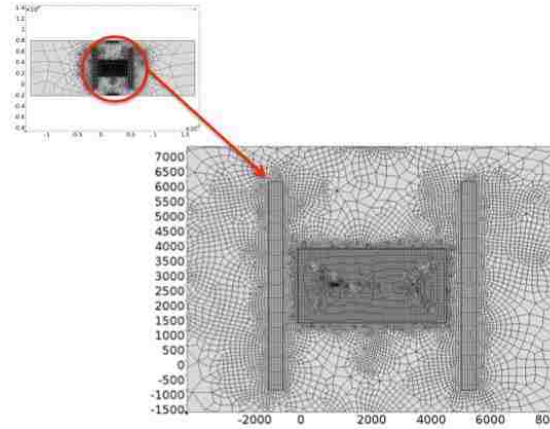


Figure 29: Mesh for model, axis in  $\mu\text{m}$ .

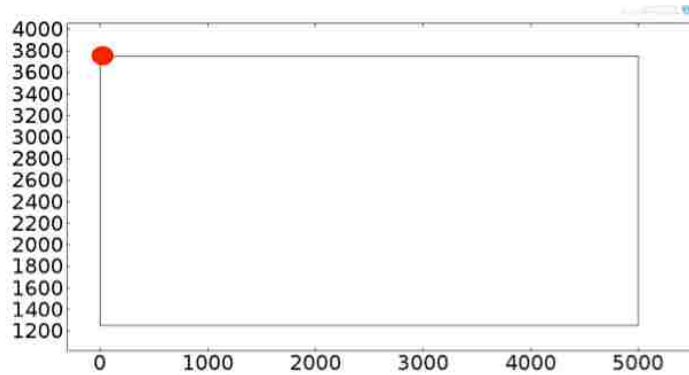


Figure 30: Cut Point for data recording, axis in  $\mu\text{m}$ .

The physics applied to this model are Magnetic Fields (No Current), Solid Mechanics, and Moving Mesh. The Magnetic Fields and the Solid Mechanics are connected to represent the MRE's ability to change its properties. The different physics and their domain conditions are shown in Figure 31 and listed in Table 7. The moving mesh is used so that the air component in the model can be excluded from the Solid Mechanics, but still considered in the calculations. The boundary conditions for Solid Mechanics are shown in Figure 32 and listed in Table 8. The force calculation from the Magnetic Fields portion is applied to three sides of the MRE to best represent the interaction between the MRE and the magnetic field.

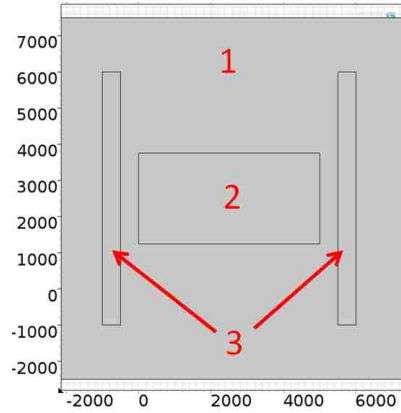


Figure 31: Domain conditions.

Table 7: Domain conditions.

Physics	Domain	Condition	Specification
Magnetic Fields, No Current	1	Magnetic Flux Conservation	Relative permeability
	3	Magnetic Flux Conservation	Magnetization: $x=B$ (parameter sweep)
		Force Calculation	Named: Fmxwl
	2	Magnetic Flux Conservation	BH curve
Solid Mechanics	2	Linear Elastic Material	N/A
Moving Mesh	1,3	Free Deformation	N/A
	2	Prescribed Deformation	N/A

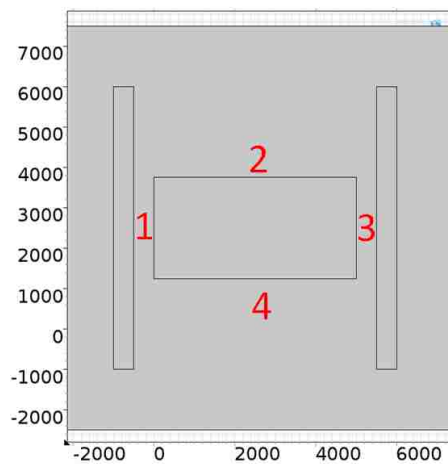


Figure 32: Boundary Conditions.

**Table 8: Boundary Conditions.**

<b>Physics</b>	<b>Boundary</b>	<b>Condition</b>
Solid Mechanics	4	Fixed
	1, 2, 3	Boundary Load: $F_x = \text{mfnc.Forcex\_ Fmxwl};$ $F_y = \text{mfnc.Forcex\_ Fmxwl}.$

#### 4.4 Results

A parameter sweep is applied to the model and run from 0 to 100,000 A/m, in steps of 10,000. The model is then run and all of the data is plotted. Figure 33 shows the values of shear modulus that were calculated using the MATLAB function. Figure 34, Figure 35, and Figure 36 show all of the plots from the model. The data from the constant shear modulus is higher than the data from the varying shear modulus. This verifies that the models are accurate because with the increasing shear modulus, the deformation decreases since the MRE is stiffer than before. The stress and strain plots also make sense for the same reason.

It can be seen that the shear modulus plot does not plateau. This may be because the MRE is not over saturated and more detailed SEM photos could be needed to get better values for the MATLAB function. None of the plots reaches a maximum and plateaus. With more intricate photos from the SEM, the values used in the function will be more accurate for each MRE sample. The photo (Figure 3) used for this function is 500 times magnified, while the ones used in the paper are 1600 times magnified. They are able to get better calculations for their measurements, which could be making their analysis more accurate.

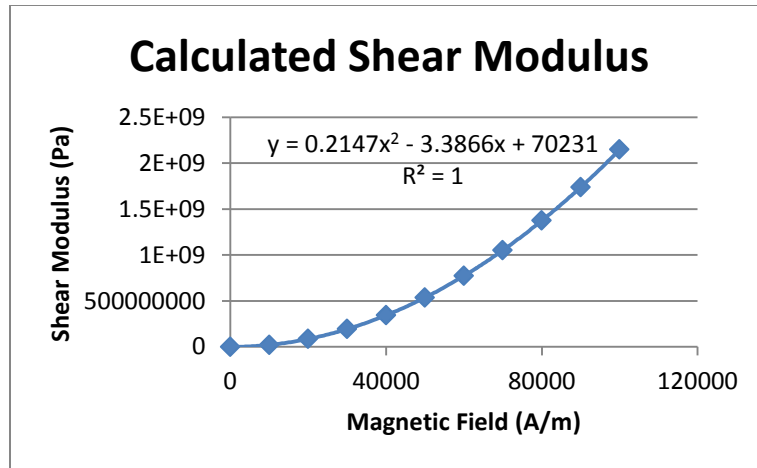


Figure 33: Calculated shear modulus using MATLAB function.

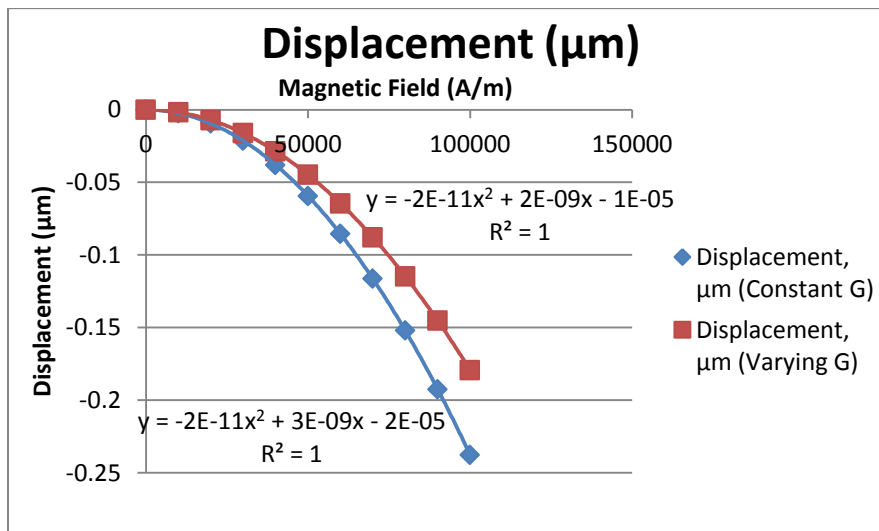


Figure 34: Displacement data.

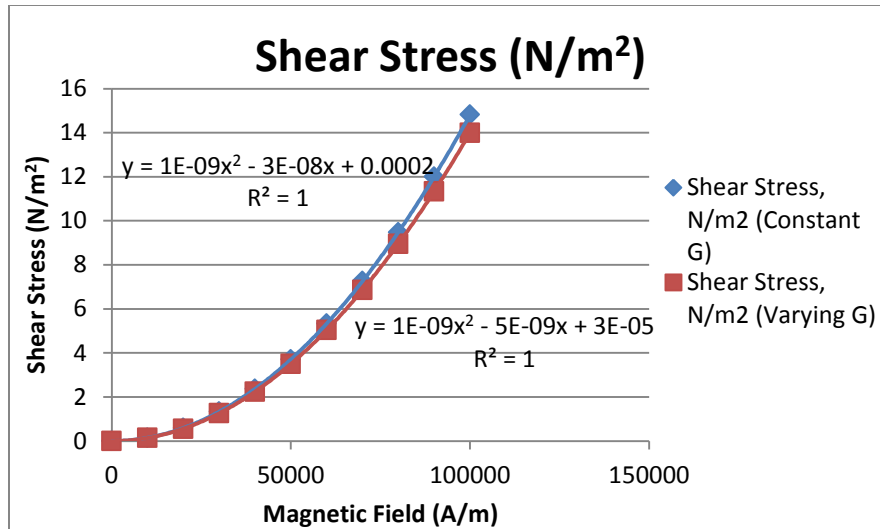


Figure 35: Shear stress data.

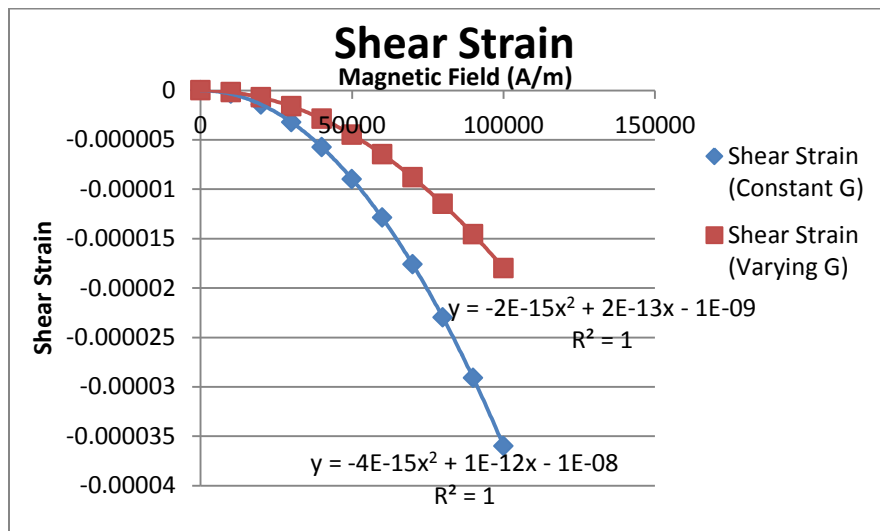


Figure 36: Shear strain data.

#### 4.5 Discussion

Overall, the model is able to connect MATLAB and COMSOL. It can be used to see how the magnetic field affects the MRE. However, some work needs to be done in more accurately calculating the shear modulus. This could be done with better SEM images as well as experimental data for the shear strain at each magnetic field used in the model. Having the shear strain can give a better simulation of the MRE and how its shear modulus changes.

## Chapter 5: Conclusions and Future Work

### 5.1 Conclusions

MRE is an evolving field. This work demonstrates some of the issues associated with the fabrication and characterization of MRE, along with how to possibly resolve them. Several combinations for manufacturing MRE were tested. The final design of the MRE material had a shear modulus that is a function of the magnetic field. To use the proposed design in haptic applications, it would be useful to increase the range of the shear modulus. This can be done by choosing a base silicone of the MRE that is not very stiff initially. Also, the curing process could be explored to tune the performance of the material.

The characterization process of the MRE using the Bose DMA has been accurate and very useful. It was verified by testing Neoprene in the same testing environment as the other samples. The DMA is able to record all of the necessary data and calculate the mechanical properties requested. The testing fixture could be used for future samples.

For the haptic device that was designed in COMSOL, the analysis was successful in creating a miniature device. The device has a toroidal permanent magnet with a 750 turn coil sitting in the middle of it. There is a core to help facilitate the motion of the field in the device. The magnetic shielding is made of 1018 steel. It is still able to produce and direct the field in the direction desired. However, the smallest magnet that had the right amount of strength is still about 3 inches in diameter, causing the device to be relatively bulky. To solve this, new ways of pre-straining the MRE could be pursued to allow further miniaturizing of the device.

COMSOL Multi-Physics was also used to develop a model that can show how the shear modulus of an MRE can change when subjected to a magnetic field. A MATLAB function is written to provide the shear modulus value as a function of the magnetic field. This function can be used to any MRE composition, as long as there are SEM photos of it. However, these photos need to be very detailed to get accurate results. The model shows that the MRE becomes stiffer and deforms less with the increasing magnetic field.

## 5.2 Future Work

It is desirable to expand the range of the shear modulus of MRE to make it useful in many applications. To achieve this, a base silicone that has a lower shear modulus is needed because if the base is already inherently stiff, it is difficult for the MRE to change its shear modulus. The MRE will probably then have a better ability to change with a new material as the base. The goal is to get at least 50% increase so that it can be felt for the haptic feedback. The current MRE has only 10%, which is difficult for a user to sense the difference in stiffness. After looking through many papers, Xiameter RTV is a silicone that is most commonly used and could be a viable option for a new MRE.

Finding a permanent magnet in a desired shape is difficult because making magnets is a very intricate process. The shape, size, and material all have an affect about the strength of the material. Having to stay with an off-the-shelf magnet causes the device to have to be built around. A way to pre-strain the MRE is to add magnetic powder into the composition, eliminating the need for permanent magnets. A coil will only be necessary for the device. It will need to be tested to see if this could work. For the experiments, barium ferrite is the magnetic powder that will be introduced into the

compositions. It is usually used for making low strength magnets (for example fridge magnets). Iron particles will be used as the active particles.

The COMSOL-MATLAB simulation will need some fine-tuning to gain results that are more accurate. To do this, higher magnification images using the SEM will be taken. This will ensure that the initial values used in the function are precise. Since the model works, it could also be useful to find other papers and develop other functions to be tested in COMSOL. By doing multiple types of analyses, they can be compared to find the most accurate model. All of these results will be compared to the experimental results.



## Appendix

### Appendix A: MATLAB Code

```
function out=shear_modulus_test(B)

H_0=B; % A/m

% Define Constants

k_i=[30 25 55 35]; % um

L=190; % um

Sigma_ki_L=sum([k_i/L]);

phi=0.15; % Volume percent of CIP

n=3; % Number of CIP, estimated through image processing of SEM

m=30e-6; % m, distance between iron columns

d=3.5e-6; % m, diameter of CIP

mu_m=2; % effective permeability of matrix

mu_p=1000; % effective permeability of CIP

f=pi/6; % particle's volume percentage in a cube particle-unit

mu_pu=mu_m+2*f*mu_m*(mu_p-mu_m)/(mu_p+mu_m-f*(mu_p-mu_m));

mu_12=((n*d)/m)^2*mu_pu+(1-((n*d)/m)^2)*mu_m;

mu_parallel=(mu_12*mu_m)/(Sigma_ki_L*mu_m+(1-Sigma_ki_L)*mu_12);

mu_b=(mu_pu*mu_m)/((n*d)/m)*mu_m+(1-(n*d)/m)*mu_pu);

mu_a=((n*d)/m)*mu_b+(1-(n*d)/m)*mu_m;

mu_perpendicular=Sigma_ki_L*mu_a+(1-Sigma_ki_L)*mu_m;

if B==0

    theta=1;

    out=0.101e6; % Pa

elseif B==10000
```

```

theta=-3.59e-07;

out=((mu_parallel-mu_perpendicular).*H_0.^2.*sin(theta).*cos(theta))./theta;

elseif B==20000

theta=-1.44e-06;

out=((mu_parallel-mu_perpendicular).*H_0.^2.*sin(theta).*cos(theta))./theta;

elseif B==30000

theta=-3.23e-06;

out=((mu_parallel-mu_perpendicular).*H_0.^2.*sin(theta).*cos(theta))./theta;

elseif B==40000

theta=-5.75e-06;

out=((mu_parallel-mu_perpendicular).*H_0.^2.*sin(theta).*cos(theta))./theta;

elseif B==50000

theta=-8.99e-06;

out=((mu_parallel-mu_perpendicular).*H_0.^2.*sin(theta).*cos(theta))./theta;

elseif B==60000

theta=-1.29e-05;

out=((mu_parallel-mu_perpendicular).*H_0.^2.*sin(theta).*cos(theta))./theta;

elseif B==70000

theta=-1.76e-06;

out=((mu_parallel-mu_perpendicular).*H_0.^2.*sin(theta).*cos(theta))./theta;

elseif B==80000

theta=-2.30e-05;

out=((mu_parallel-mu_perpendicular).*H_0.^2.*sin(theta).*cos(theta))./theta;

elseif B==90000

theta=-2.91e-05;

out=((mu_parallel-mu_perpendicular).*H_0.^2.*sin(theta).*cos(theta))./theta;

```

```
else B==100000  
    theta=-3.60e-05;  
    out=((mu_parallel-mu_perpendicular).*H_0.^2.*sin(theta).*cos(theta))./theta;  
end
```

## Bibliography

- Chen, L., Gong, X. L., & Li, W. H. (2007). Microstructures and viscoelastic properties of anisotropic magnetorheological elastomers. *Smart Materials and Structures*, 16(6), 2645–2650. doi:10.1088/0964-1726/16/6/069
- Ham, R. V. A. N., Sugar, T. G., Vanderborght, B., Hollander, K. W., & Lefeber, D. (2009). Review of Actuators with Passive Adjustable Compliance/Controllable Stiffness for Robotic Applications, (September), 81–94.
- Kallio, M. (2005). *The elastic and damping properties The elastic and damping properties*. Tampere University of Technology.
- Kosasih, P. B., Liu, B., Li, W. H., & Zhang, X. Z. (2006). Development of an MR-brake-based haptic device. *Smart Materials and Structures*, 15(6), 1960–1966. doi:10.1088/0964-1726/15/6/052
- Li, W., & Zhang, X. (2008). Research and Applications of MR Elastomers. *Recent Patents on Mechanical Engineering*, 1(3), 161–166. doi:10.2174/2212797610801030161
- Liao, G., Gong, X., Xuan, S., Guo, C., & Zong, L. (2012). Magnetic-Field-Induced Normal Force of Magnetorheological Elastomer under Compression Status. *Industrial & Engineering Chemistry Research*, 51(8), 3322–3328. doi:10.1021/ie201976e
- Opie, S. (2008). DESIGN AND CONTROL OF A VIBRATION ISOLATOR USING A BIASED, (December).
- Opie, S., Yun, H., & Yim, W. (2012). Impact Mitigation of Robotic System using Variable Stiffness Joints, (Urai 20), 395–397.
- Park, S. (2008). Design of a robot joint with variable stiffness. In *2008 IEEE International Conference on Robotics and Automation* (pp. 1760–1765). Pasadena: IEEE. doi:10.1109/ROBOT.2008.4543455
- Ruddy, C., Ahearne, E., & Byrne, G. (2012). A review of magnetorheological elastomers: properties and applications. ... *Science (AMS) Research*. [Http://www. Ucd. Ie](http://www.Ucd.Ie) ... Retrieved from [http://www.ucd.ie/mecheng/ams/news\\_items/Cillian Ruddy.pdf](http://www.ucd.ie/mecheng/ams/news_items/Cillian_Ruddy.pdf)
- Wolf, S., & Hirzinger, G. (2008). A new variable stiffness design: Matching requirements of the next robot generation. *2008 IEEE International Conference on Robotics and Automation*, 1741–1746. doi:10.1109/ROBOT.2008.4543452

## Curriculum Vitae

### Sarah Trabia

<b>Institution</b>	<b>City and State</b>	<b>Degree</b>	<b>Area of Concentration</b>	<b>Month/Year Received</b>
University of Nevada, Las Vegas	Las Vegas, Nevada	Ph.D. in Mechanical Engineering	Dynamics and Controls	May 2017 (Expected)
University of Nevada, Las Vegas	Las Vegas, Nevada	M.S. in Mechanical Engineering	Dynamics and Controls	July 2014 (Expected)
University of Nevada, Las Vegas	Las Vegas, Nevada	B.S. in Mechanical Engineering		December 2012

### Honors and Awards

- Received a \$13,000 NASA fellowship, Spring '14
- Continuously on the Dean's List since joining UNLV
- Graduated with the highest GPA in Mechanical Engineering
- Magna Cum Laude, University Honors, Department Honors
- Chosen as Outstanding Graduate for the Bachelors Graduating Class of Fall '12 and for the Department of Mechanical Engineering
- Member of Tau Beta Pi and Phi Kappa Phi honor societies
- EIT (Engineer in Training) Certified since May 2011

### Relevant Experience

<b>Dates</b>	<b>Position</b>
2013 - present	Graduate Assistant Department of Mechanical Engineering, University of Nevada, Las Vegas, Las Vegas, Nevada <ul style="list-style-type: none"> <li>• Developed a device that uses magnetic field to control the stiffness of Magnetorheological elastomers.</li> <li>• Taught Engineering Measurements and Automatic Controls undergraduate labs.               <ul style="list-style-type: none"> <li>○ Duties include developing lab manuals</li> <li>○ Both courses use LabVIEW and Simulink software packages as well as their integration with NI hardware.</li> </ul> </li> </ul>
2012 – 2012	Mechanical Engineering Intern Varian Medical Systems, Las Vegas, Nevada <ul style="list-style-type: none"> <li>• Participated in developing models for multiple components of X-ray detectors for cargo inspection using Pro-E</li> <li>• Conducted Finite Element Analysis, Pro-Mechanica, of the current frame for an X-ray detector, Linatron M.</li> <li>• Performed weight optimization for the Linatron M.</li> </ul>

- 2011 - 2011      Research Assistant  
Center for Materials and Structures, University of Nevada, Las Vegas,  
Las Vegas, Nevada
- Tested composite cylinders for compressive strength at room and elevated temperatures (400°F and 750°F). We also did experiments to measure the coefficient of thermal expansion.
  - Assisted in extracting displacement data from high speed videos for a composite blast containment vessel experiment.

### **Other Experience**

- | Dates          | Position                            |
|----------------|-------------------------------------|
| 2011 - present | Mentor for local FTC® team, Area 52 |
- Coached the students in designing a robot for the year's game
  - Assist in troubleshooting
  - Explain Mechanical Engineering concepts

### **Publications**

Trabia, S., Hwang, T., & Yim, W. (2014, March). Programmable variable stiffness 2D surface design. In *SPIE Smart Structures and Materials+ Nondestructive Evaluation and Health Monitoring* (pp. 90580X-90580X). International Society for Optics and Photonics.

### **Presentations**

“Programmable variable stiffness 2D surface design”  
SPIE Smart Structures and Materials, March 11, 2014. San Diego, CA.

Variable stiffness features can contribute to many engineering applications ranging from robotic joints to shock and vibration mitigation. In addition, variable stiffness can be used in the tactile feedback to provide the sense of touch to the user. A key component in the proposed device is the Biased Magnetorheological Elastomer (B-MRE) where iron particles within the elastomer compound develop a dipole interaction energy. A novel feature of this device is to introduce a field induced shear modulus bias via a permanent magnet which provides an offset with a current input to the electromagnetic control coil to change the compliance or modulus of a base elastomer in both directions (softer or harder). The B-MRE units can lead to the design of a variable stiffness surface. In this preliminary work, both computational and experimental results of the B-MRE are presented along with a preliminary design of the programmable variable stiffness surface design.

### **Recent / Current Research**

Current research is being conducted on Magnetorheological elastomers (MRE). This includes both the analytical using COMSOL and experimental. The material is made and then tested in a Bose Dynamic Mechanical Analyzer to find their mechanical characteristics.